ORIGINAL RESEARCH

Exploring the Mechanisms of Modified Bu-Shen-Yi-Qi Decoction for COPD-Related Osteoporosis Therapy via Transcriptomics and Network Pharmacology Approach

Yuanyuan Zhong[1,2], Bin Wang[1,2], Wenjing Chen[1,2], Hongying Zhang[1,2], Jing Sun[1,2], Jingcheng Dong [1,2]

[1]Department of Integrative Medicine, Huashan Hospital, Fudan University, Shanghai, People's Republic of China; [2]Institute of Integrated Traditional Chinese and Western Medicine, Huashan Hospital, Fudan University, Shanghai, People's Republic of China

Correspondence: Jingcheng Dong; Jing Sun, Email jcdong2004@126.com; sjing0610@163.com

Purpose: To investigate the effectiveness of modified Bu-Shen-Yi-Qi decoction (MBSYQ) in the treatment of osteoporosis associated with chronic obstructive pulmonary disease (COPD) and its underlying mechanisms of action.

Methods: Disease targets, active ingredients and targets were predicted by TTD, CTD, DisGeNET, HERB (BenCaoZuJian as its Chinese name), and multiple-TCM databases; In addition, the screened targets were performed via the online platforms DAVID 6.8 and Metascape for GO and KEGG pathway enrichment analysis; The relationship between the MBSYQ and core targets were verified by molecular docking technique. Then we established a COPD-associated osteoporosis rat model by passive 24-week cigarette exposure. We assessed the efficacy of MBSYQ by lung histopathology assessment and distal femur/the first lumbar vertebra (L1) microstructural assay. In addition, we performed tibial RNA sequencing, which was validated by RT-PCR and Western blot.

Results: Screening revealed that the 350 active compounds of MBSYQ anchored 228 therapeutic targets for COPD-related osteoporosis; KEGG pathway enrichment analysis showed that the key targets mainly regulated MAPK and PI3K/AKT signaling pathways. In vivo studies showed that MBSYQ treatment alleviated pathological alterations in lung tissue, and reversed the bone loss and microstructure damage in the femur/L1 of model rats. The RNA seq indicated that MBSYQ could upregulate genes associated with anti-oxidative stress and aerobic respiration. The GSEA analysis displayed that MAPK and PI3K/AKT pathways were inhibited by CS exposure and activated by MBSYQ.

Conclusion: MBSYQ is effective in the prevention and treatment of COPD-related osteoporosis, partially achieved by improving oxygen metabolism and activating MAPK and PI3K/AKT pathways.

Keywords: COPD, osteoporosis, modified Bu-Shen-Yi-Qi formulae, network pharmacology, transcriptomics

Introduction

Data show that the third leading cause of death worldwide is caused by chronic obstructive pulmonary disease (COPD).[1] It's a common, preventable and treatable chronic respiratory disease characterized by incomplete reversibility and progressive airflow limitation. COPD is often associated with comorbidities and systemic consequences, including lung cancer, muscle weakness, osteoporosis, and further decreases the quality of life and increases mortality.[2–4] Patients with COPD are significantly more likely to develop osteoporosis than healthy individuals, and its severity is strongly associated with a decrease in bone mineral density (BMD).[5–10] In addition, the most common cause of secondary osteoporosis in men may be due to COPD.[11]

Chronic airway inflammation, characterized by inflammatory cell infiltration and increased secretion of inflammatory mediators, is thought to be the main cause of the ongoing progression of COPD.[12] Osteoporosis is generally characterized by low bone mass, microarchitectural degeneration, and increased fracture risk.[13] Although the prevalence of osteoporosis is significantly increased in patients with COPD compared to normal people, the causal and molecular links between them

2727

remain unclear.[14] It is difficult to clarify the pathological mechanism because of the various factors that affect bone metabolisms, such as smoking, weight, COPD acute exacerbation, sarcopenia, steroid use, etc.[15] To make matters worse, COPD-related osteoporosis is highly neglected by respiratory and physicians, and no formal guidelines for managing COPD-associated osteoporosis.[2,16,17] Due to the paucity of specific evidence in COPD patients, treatment is generally guided by the practice guidelines for primary osteoporosis. Current treatments include interventions for patients' lifestyles (moderate exercise, healthy diet, etc.) and pharmacological treatments (calcium and vitamin D supplementation, etc.), selective estrogen receptor modulators, RANKL inhibitors, calcitonin, bisphosphonates, and PTH receptor agonists, etc.[18] However, it's limited in its efficiency in restoring bone loss or increasing bone mass and has unavoidable side effects.[19] Mesenchymal stem cell transplantation is thought to be a novel treatment for osteoporosis. However, it is still in preclinical studies and clinical trials, and its safety and efficacy need to be further evaluated.[20,21]

Traditional Chinese Medicine (TCM) is an integrated system of medicine that has played an important role in the maintenance of people's health worldwide for thousands of years.[22,23] The efficacy of TCM has been proven to be a viable alternative therapy for the treatment of diseases.[24] Bu-Shen-Yi-Qi decoction, composed of three herbs including Epimedium brevicornum Maxim. (Epimedii Herba), Astragalus mongholicus Bunge (Radix Astragali), and Rehmannia glutinosa (Gaertn.) DC. (Radix Rehmanniae), have been proven effective in clinical and experimental studies for the treatment of chronic respiratory diseases such as asthma and COPD.[25–28] Our previous randomized, double-blinded, multicenter clinical trial demonstrated that it improved lung function, reduced the frequency of acute exacerbations, and attenuated the inflammation response in COPD patients.[27] In addition, a modified version of the Bu-Shen-Yi-Qi formulae (MBSYQ, Scutellaria baicalensis Georgi (Radix Scutellariae) and Paeonia lactiflora Pall. (Radix Paeoniae Rubra) were added, detailed in Table S1) is more effective in treating acute exacerbations of COPD, such as shortness of breath and relief of cough.[29] However, it remains unclear whether MBSYQ is effective in the prevention and treatment of COPD-related osteoporosis.

We first explored the potential molecule link between COPD and osteoporosis from the perspective of network pharmacology, the possible mechanisms of MBSYQ for COPD-related osteoporosis treatment, and then established a 24-week CS-induced animal model to validate the pathological mechanisms, influencing factors and underlying mechanisms of MBSYQ for COPD-related osteoporosis treatment, which can provide further clinical applications and basic research. The study design is displayed in Figure 1

Materials and Methods
COPD & Osteoporosis-Related Protein Screening
Therapeutic Target Database (TTD, http://bidd.nus.edu.sg/group/cjttd/)[30] and Comparative Toxicogenomics Database (CTD, http://ctdbase.org/)[31] can be used to screen target proteins for COPD and osteoporosis; Potential targets for COPD and osteoporosis were collected by DisGeNET database (https://www.disgenet.org/).[32] We searched all three databases using the keywords "Chronic obstructive pulmonary disease" or "Osteoporosis" and set the species to "Homo sapiens". Finally, we removed duplicates and integrated all information to further analyze proteins common to COPD and osteoporosis.

Bioactive Ingredients Collection and Target Prediction
Potentially active compound screening and candidate target prediction for MBSYQ were screened from the HERB database (BenCaoZuJian as its Chinese name, obtained from http://herb.ac.cn/) which links 12,933 targets and 28,212 diseases to 7263 herbal medicines and 49,258 ingredients. They provided six pairwise relationships between them by integrating multiple-TCM databases (SymMap, TCMID 2.0, TCMSP 2.3, and TCM-ID) and manually 1966 reference comparisons.[33] We further searched SuperTarget (https://bioinformatics.charite.de/supertarget/),[34] SwissTargetPrediction (www.swisstargetprediction.ch),[35] Similarity ensemble approach (SEA, https://sea.bkslab.org/),[36] STICH (http://stitch.embl.de/)[37] and PharmMapper (http://www.lilab-ecust.cn/pharmmapper/)[38] databases for component-target prediction of icaritin and astragaloside IV. Networks were built and visualized with Cytoscape 3.8.0.[39] Network parameters were calculated by the NetworkAnalyzer plugin.
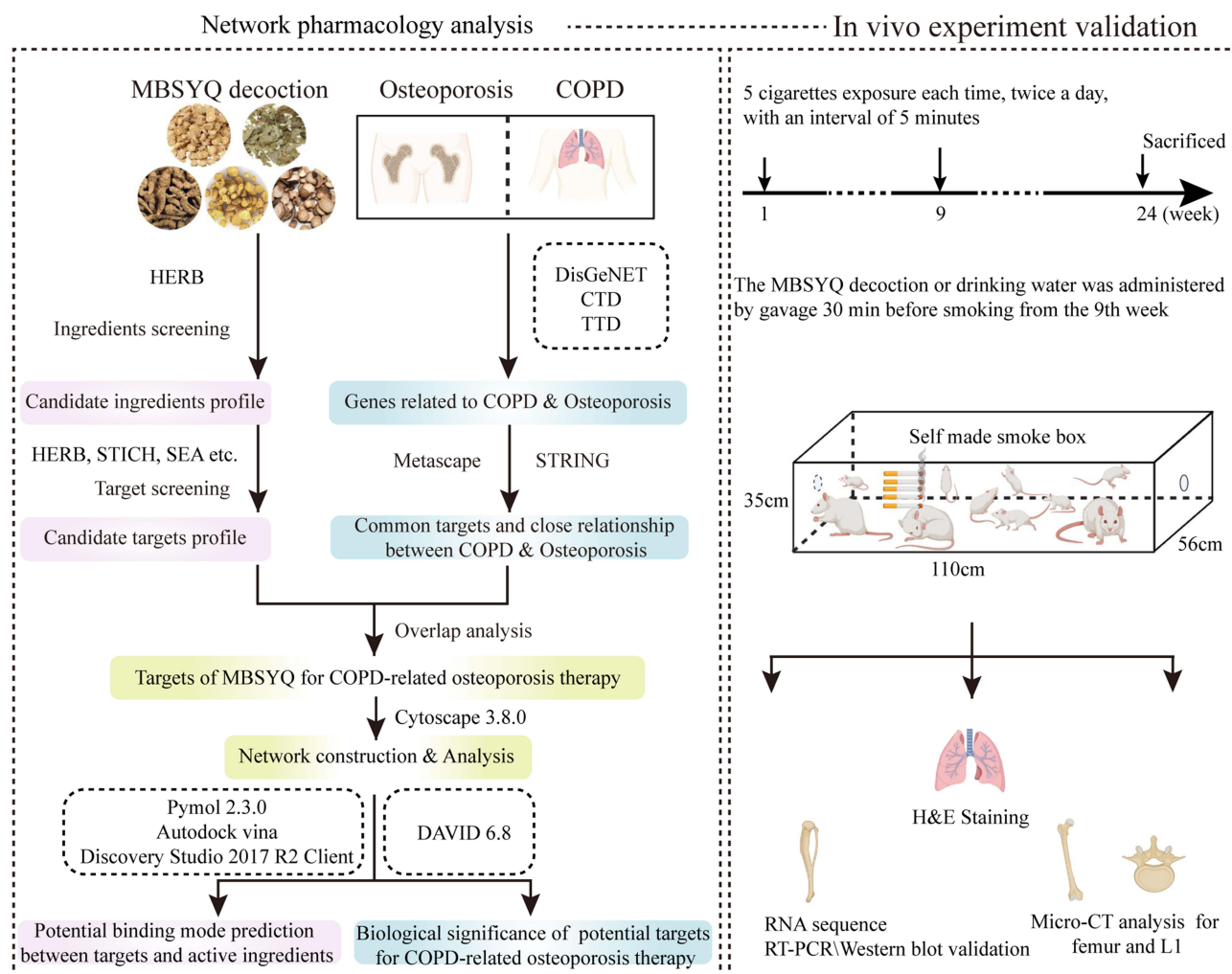
Figure 1 Schematic diagram of the study to explore the pharmacological mechanisms of MBSYQ in COPD-related osteoporosis.

Gene Ontology (GO) and Pathway Enrichment Analysis

To further reveal the mechanism of MBSYQ for COPD-related osteoporosis, through the online platforms DAVID 6.8 (https://david.ncifcrf.gov/)[40] and Metascape (https://metascape.org/),[41] the targets of MBSYQ for COPD-related osteoporosis therapy were additionally analyzed by GO and KEGG pathway enrichment.

Molecule Docking

Three-dimensional chemical structures of the core active ingredients were obtained from the PubChem database (NCBI, USA), and energy minimized by molecular mechanics-2 (MM2) force fields in Chem 3D Pro; The RCSB Protein Data Bank (www.rcsb.org) was used to retrieve the crystal structures of the target proteins; The AutoDock tool (1.5.6) was performed for the addition of hydrogen atoms and the removal of water and heterogeneous molecule; AutoDock vina was employed to predict potential molecular binding patterns between components and candidate targets; the docked structures were analyzed via PyMol 2.3.0 (http://www.pymol.org/). The position of the original ligand defines the center of the active site for protein-ligand docking, set to a grid size of $40 \times 40 \times 40$ Å in the x, y, and z directions, with the spacing between the two grid points set to 0.375 Å. The most likely binding mode is the docking conformation corresponding to the lowest binding energy.

Chemicals and Reagents

Primary antibodies against P-JNK (4668T), P-ERK (4370), P-P38 (4511T), and β-actin (4970) were from Cell Signalling Technology (Danvers, USA). Anti-P-Akt (66444-1-Ig) was obtained from Proteintech. Commercial tobacco Daqianmen was purchased from Shanghai Jieqiang Tobacco, Sugar and Wine (Group) Co., Ltd.

MBSYQ Preparation

MBSYQ granules were purchased from Jiangyin Tianjiang Pharmaceutical Co., Ltd. Briefly, the herbs were decocted twice with water, then filtered and concentrated to a relative density of 1.11–1.13 (Astragalus mongholicus Bunge), 1.09–1.11 (Epimedium brevicornu Maxim.), 1.09–1.12 (Rehmannia glutinosa (Gaertn.) DC.), 1.15–1.17 (Scutellaria baicalensis Georgi) and 1.05–1.07 (Paeonia lactiflora Pall.) at 65±5°C, respectively. The herbal extracts were obtained by spray drying with 18–40 mesh screening and then quality controlled by ultraviolet-visible spectrophotometry (UU-Vis) and high-performance liquid chromatography (HPLC). The pellets of each herb were mixed in proportion and diluted with potable water before administration.

Animal Model and Treatment

Selected 40 male SD rats (6 weeks old, 160–200 g) (Sippr-BK Laboratory Animals Co. Ltd., Shanghai, China) and housed in a specific pathogen-free (SPF) condition under a 12: 12 h light-dark cycle and given free access to food and water. Animal experiments were approved by the Animal Experimentation Ethics Committee of Fudan University (Approval No. 202011005S). Rats were acclimated to the conditions for one week before the experiment and randomly divided into five groups (n = 8 per group): Normal control group, CS group, CS + MBSYQ low/medium/high dose group (6.25 g/kg, 12.5 g/kg, 25 g/kg). The medium doses given to rats were calculated based on the animal dose conversion table and body surface area.[42] Construction of rat model of chronic obstructive pulmonary disease with slight modifications from references.[43–45] Briefly, rats were placed in a homemade acrylic chamber (110 × 56 × 35 cm) and exposed to smoke from 5 cigarettes (commercial cigarettes, large front door, each containing 12 mg carbon monoxide, 9 mg tar, and 0.8 mg nicotine) (30 min each, twice a day, 5 min smoke-free interval, 6 days a week for 24 weeks), except for normal controls. Beginning at week 9, rats were gavaged with different doses of MBSYQ decoction or the same volume of drinking water 30 min before CS exposure.

Lung Histopathology Detection and Evaluation

The right middle lobe of the rat lung was excised and fixed in 4% paraformaldehyde. Samples were paraffin-embedded and cut into 4 μm sections for H&E staining. The degree of infiltration of inflammatory cells in the lung was assessed according to a scoring system on a 5-point scale according to the method described by previous authors.[46] Mean linear intercept (MLI) and mean alveolar area (MAA) were used to measure airspace enlargement according to the described protocol.[47]

Micro-CT Imaging

The right femur and L1 were removed and separated from the soft tissues, scanned with QuantumGX (PerkinElmer, USA) (90kv, 88uA), and then reconstructed in 3D. The region of interest (ROI) was defined as 150 consecutive slides (3 mm) proximal to the distal femoral growth plate. Bone surface to bone volume (BS/BV), bone volume to total volume (BV/TV), connective tissue density (Conn.D), trabecular number (Tb.N), trabecular separation (Tb.Sp), and trabecular thickness (Tb.Th) were calculated by Analyze12.0.

RNA Sequence

Total RNA from the right femur was extracted according to the TRIzol kit (Invitrogen, Carlsbad, CA, USA). NanoDrop ND-1000 (NanoDrop, Wilmington, DE, USA) to quantify RNA; Bioanalyzer 2100 (Agilent, CA, USA) to evaluate RNA integrity. Eligible RNA samples were used to construct cDNA libraries. Then End-sequencing by Illumina Novaseq™ 6000 (LC-Bio-Technology CO., Ltd., Hangzhou, China) (PE150). The mRNA expression levels were performed by calculating FRKM in StringTie (FPKM = [total_exon_fragments / mapped_reads (millions) × exon_length (kB)]).

Differentially expressed genes (DEGs) with fold change > 1.5 or fold change < 0.66 were selected by the R package edgeR (https://bioconductor.org/packages/release/bioc/html/edgeR.html), and nested linear models were compared by parametric F-test (p-value <0.05). Bioinformatics analysis and PPI network construction were performed as described previously. GSEA software (Broad Institute's) (http://software.broadinstitute.org/gsea/index.jsp) for genomic enrichment analysis (GSEA).

Real Time-PCR Analysis

500ng RNA was reverse transcribed into cDNA for each sample using the PrimeScript™RT Master Mix (Takara, RR036A). The cDNAs were amplified using Genious 2X SYBR Green Fast qPCR Mix (ABclonal, RK21206) with a Real-time PCR instrument (QuantStudio 6 Flex, ThermoFisher, USA) following the manufacturer's instructions. The β-actin gene was chosen as an internal reference, and the expressions of target genes were calculated using the comparative CT method ($2^{-\Delta\Delta CT}$). The sequences of primers used are shown in Table S2. The RT-PCR assays were conducted in three independent technical replicates for each sample.

Western Blot

Total protein was extracted from the right tibia with RIPA (Beyotime, P0013B) added to a mixture of protease inhibitors and phosphatase inhibitors (Beyotime, P1050), and quantified with a BCA kit (Beyotime, P0012). The tissue lysates were mixed with 5 x SDS sample buffer (4:1, Beyotime, P0015) and heated at 99°C for 10 min. Proteins (20 μg total protein) were subsequently separated by 10% SDS-PAGE (Beyotime) and then transferred to PVDF membranes (Millipore). Blocking was performed with 5% skim milk at room temperature for 1 h. The blocking buffer solution consisted of Tween-20 (TBST) and Tris-buffered saline. The membranes were then incubated overnight with 1:1000 dilutions of primary antibodies against β-actin, P-AKT, p-ERK, p-P38, and p-JNK. The membranes were washed three times with TBST before incubation with 1:10000 dilution of HRP-conjugated secondary antibody (Proteintech) for 1 h, and the ECL detection system visualized the membranes with an enhanced chemiluminescence kit (Millipore, Billerica, USA). β-actin was used as an internal control. Bands were scanned using Image-Pro Plus 6.0 and quantitated by densitometry.

Statistical Analysis

Data were expressed as mean ± SD. One-way ANOVA and LSD multiple comparison tests were performed using Prism 6.0 (GraphPad, La Jolla) to assess between-group differences when homogeneity of variance and normality were satisfied. Otherwise, Dunnett's T3 and nonparametric tests were performed. P value <0.05 means statistically significant.

Results
COPD and Osteoporosis-Related Proteins Collecting and Analyzing

In total, 792 COPD-related targets and 1112 osteoporosis-related targets were retrieved (Table S3) and further submitted to STRING to establish COPD and osteoporosis disease-specific protein interaction (PPI) network, respectively (Figure S1A and B). There are 340 overlapping proteins in both protein lists, and their relative positions in the protein interaction networks of COPD and osteoporosis are shown in (Figure S1C and D). We found that nodes with greater intergenic centers had greater extent in both COPD and osteoporosis disease-specific PPI networks (Figure S2A and B). Therefore, we screened the top 15 COPD and osteoporosis disease-specific proteins based on the degree values (Figure S2C and D). Among them, TP53, AKT, TNF, MAPK3, IL-6, STAT3 and EGFR, etc. occupy a central position in the disease-specific protein interaction network of COPD and osteoporosis, indicating that they play a critical role in the development and progression of both diseases. Most COPD-associated proteins belonged to the same statistically significant GO terms as osteoporosis-specific proteins (Figure 2A–D), indicating a strong functional association in these two contrasting cohorts and allowing further analysis of these 340 common proteins.
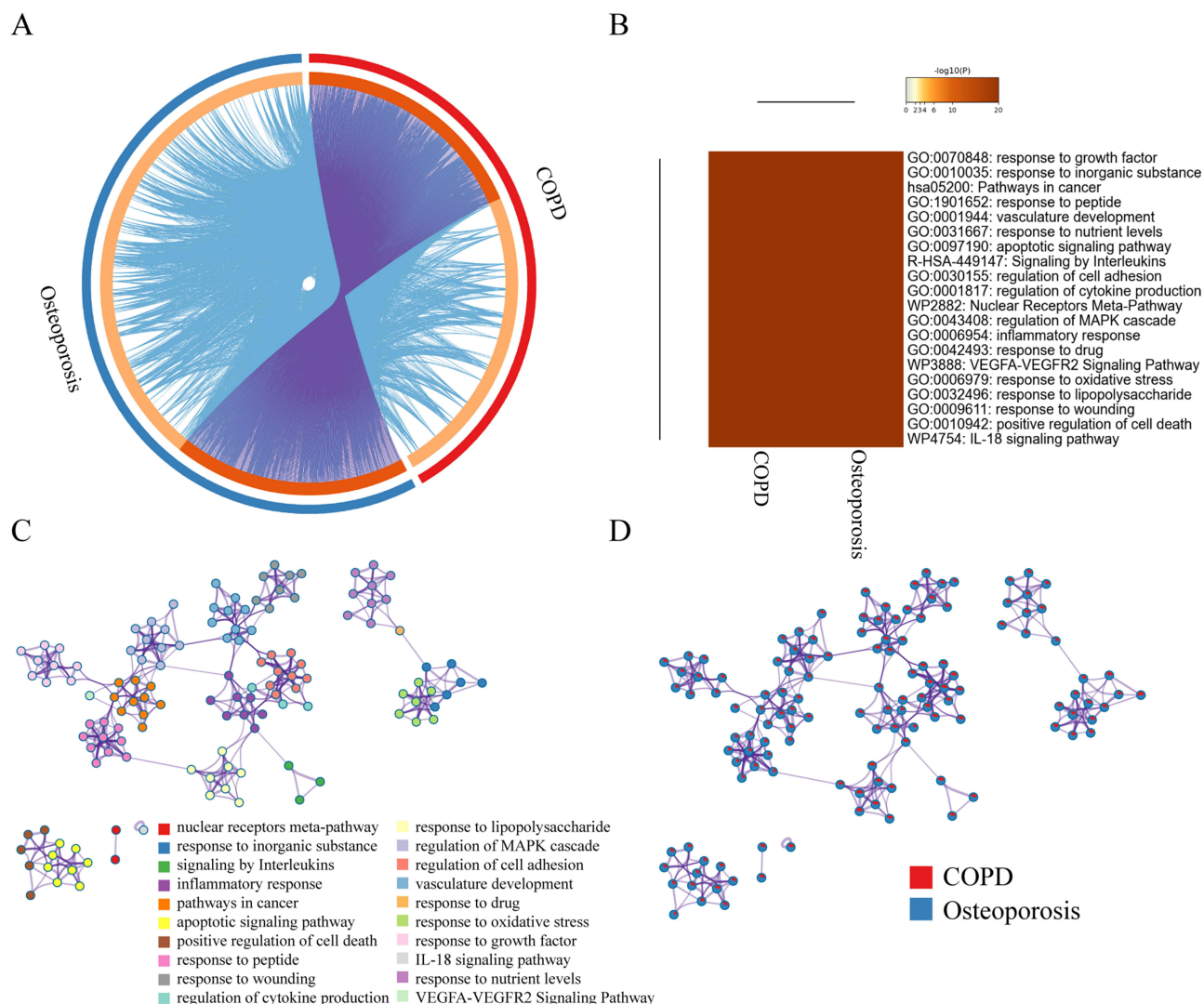
Figure 2 Co-bioinformatics analysis of the target of MBSYQ and 340 proteins in common between COPD & osteoporosis by Metascape. (**A**) Circos diagram of the 2 sets of proteins. The proteins appearing in the two sets of protein profiles are connected by purple lines, and proteins of the same ontological term are connected by blue lines. (**B**) The top 20 common GO terms or pathways enriched by 2 groups of protein profiles. (**C**) Enrichment network analysis of the 2 groups of proteins. A circular node represents a term whose size is proportional to the number of proteins, and the color represents the characteristics of the protein. When the similarity is greater than 0.3, it is connected by an edge, at which point the thickness of the edge represents the similarity. (**D**) In the enrichment network, nodes are represented as pies, and the sector of the pie is proportional to the hits in the 2 lists.

Screening of Active Ingredients of MBSYQ Decoction and Prediction of Its Action Targets

398 active ingredients and 2010 corresponding targets were retrieved (Table S4). Cytoscape 3.8.0 was used to build and analyze Herb-Ingredient-Target (H-I-T) network (Figure S3A). The H-I-T network consists of 2413 nodes (5 herbs, 398 ingredients, and 2010 targets) and 8907 edges. The molecular mechanism of MBSYQ for COPD-related osteoporosis was further explored, and we intersected the target profile of MBSYQ with 340 proteins common to COPD and osteoporosis. Finally, we retrieved 228 potential targets and considered them as potential targets for COPD-associated osteoporosis treatment. The herb-potential ingredient-potential target (HB-PI-PT) network was then built and analyzed (Figure S3B). The HB-PI-PT network consists of 583 nodes (5 herbs, 350 ingredients, and 228 targets) and 3061 edges. The core objectives and potential components of the two network parameters are shown in Figure S3C and D. Capsaicin, quercetin, eugenol, apigenin, icaritin, etc., are potential core components, and PTGS2, AR, NOS2, ESR1, PPARG, etc. are the main potential targets of MBSYQ for the treatment of COPD-related osteoporosis. Then, we performed GO and KEGG analysis on these

228 potential targets (Figure 3A–C). We found that these 228 potential targets are mainly involved in regulating apoptotic processes, inflammatory and hypoxia responses, nitric oxide biosynthesis, smooth muscle cell proliferation, etc. KEGG pathway analysis revealed that the TNF signaling pathway, toll-like receptor signaling pathway, foxo signaling pathway, HIF-1 signaling pathway, MAPK, and PI3K/AKT signal pathway, etc., are enriched and regulated by MBSYQ, suggesting a comprehensive mechanism for MBSYQ treatment of COPD-associated osteoporosis.

Potential Components and Targets of MAPK and PI3K/AKT Signaling Pathway Regulation by MBSYQ Decoction

Based on the KEGG enrichment results, we further constructed a potential target-pathway network (Figure 4A) and a potential component-potential target (PI-PT) network (Figure 4B). We found that 314 active components in MBSYQ,
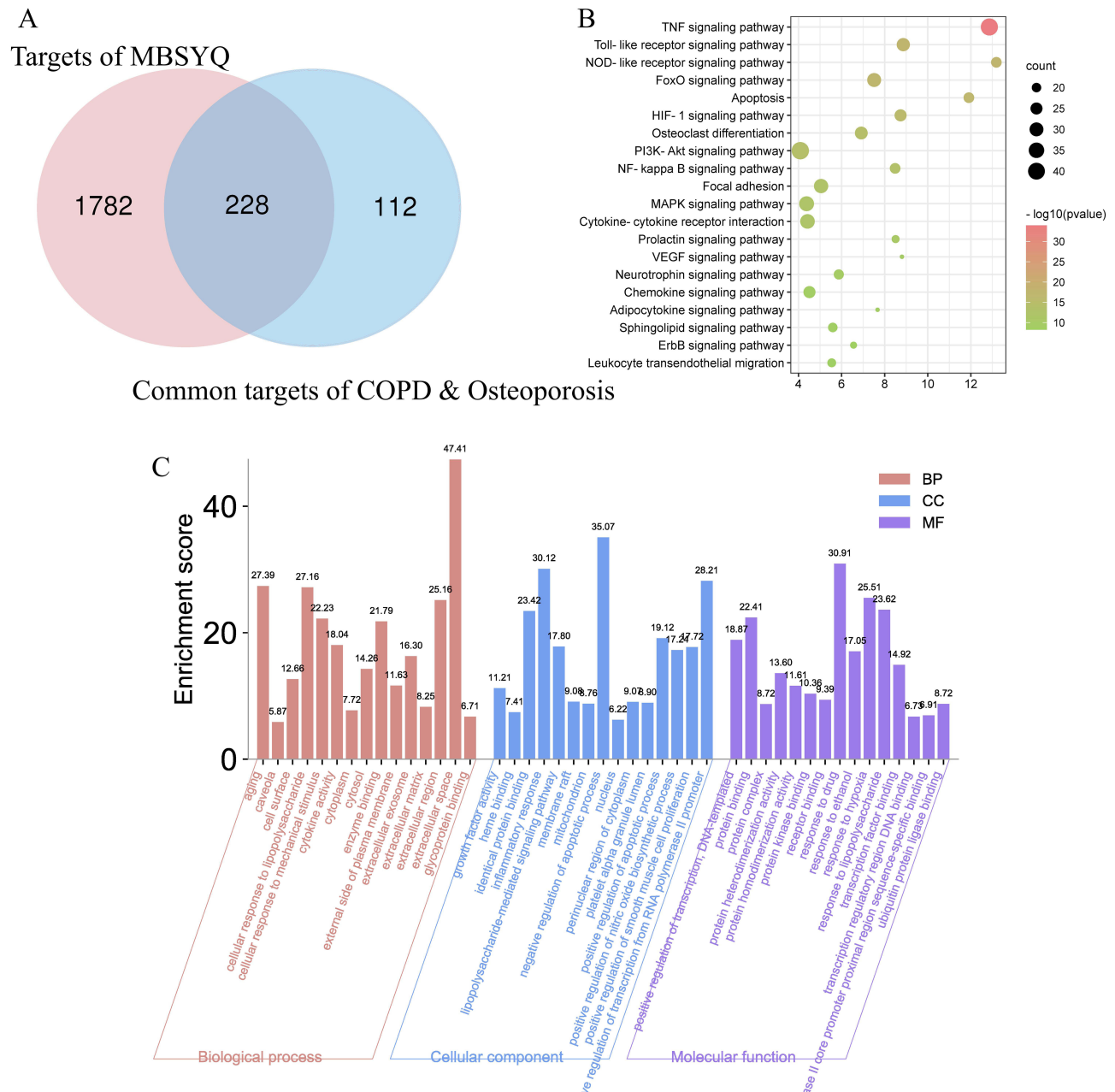
Figure 3 GO and KEGG analysis of potential components and targets of MBSYQ for COPD-associated osteoporosis by DAVID 6.8. Venn diagram of the 340 common protein profiles of MBSYQ with COPD and osteoporosis (**A**). Enrichment of the first 30 pathways of the KEGG pathways among 228 potential targets (**B**). The first 15 items of the rich GO program include biological processes (BP), cellular compartments (CC), and molecular functions (MF) (**C**).
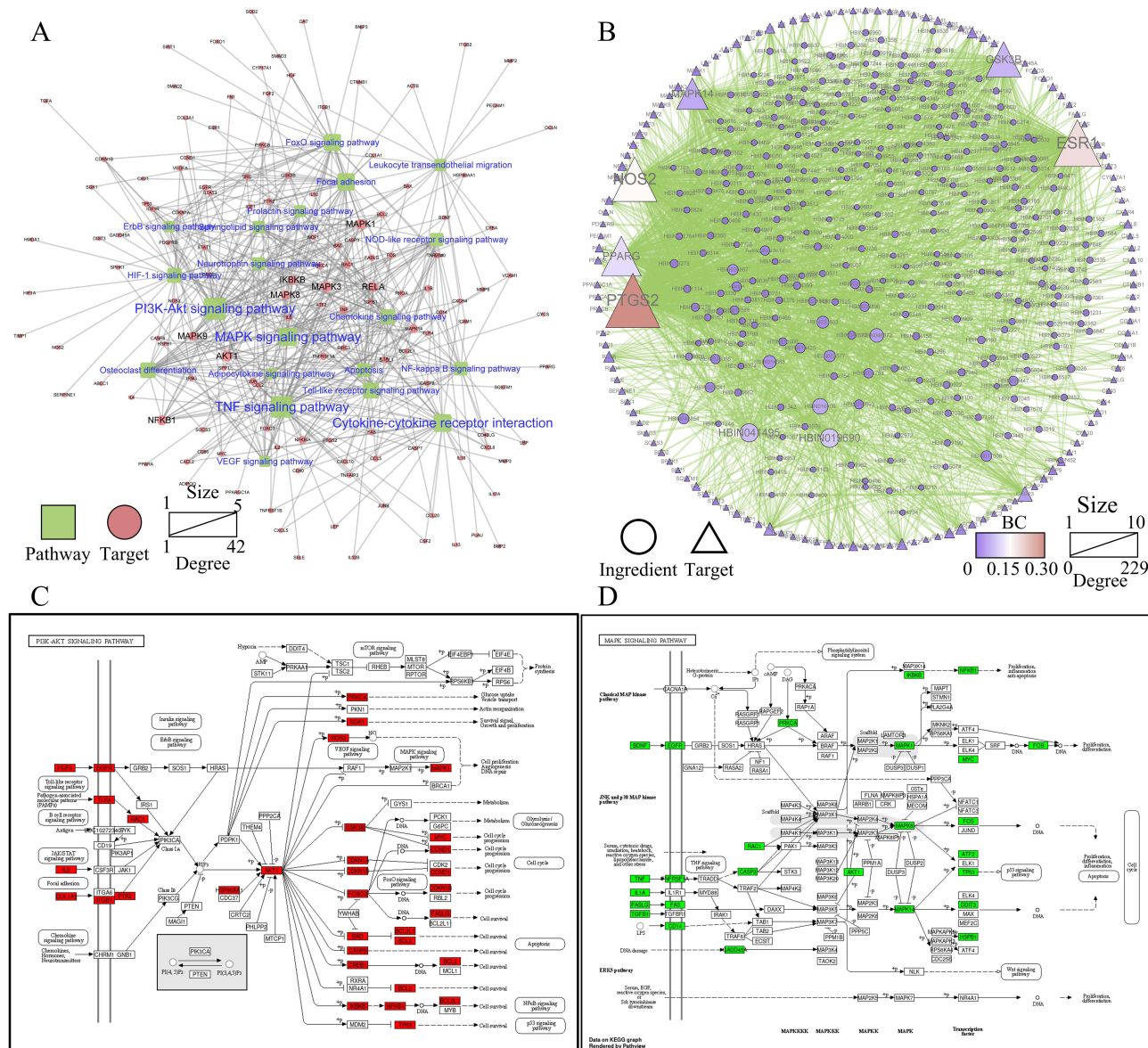
Figure 4 MBSYQ potential target-pathway (PT-P) network and potential component-potential target (PI-PT) network for COPD-related osteoporosis treatment. (**A**) PT-P network is based on the first 20 KEGG-enriched pathways. (**B**) PI-PT network based on PT-P network. (**C**) Relative positions of potential MBSYQ targets in the PI3K/AKT pathway. (**D**) Relative positions of potential targets of MBSYQ in MAPK pathway.

including quercetin, anchored 137 targets and regulated more than 20 signal pathways. Through network analysis, we found that PI3K/AKT and MAPK signaling pathways occupied relatively important positions, suggesting that they play an important role in the MBSYQ treatment of COPD-related osteoporosis. Subsequently, we labeled the relevant targets of MBSYQ regulating PI3K/AKT signaling pathway and MAPK signaling pathway (Figure 4C and D) and constructed the compound-target-pathway network (Figure 5A). 6 core compounds are shown, including quercetin, apigenin, capsaicin, aconitine, salicylic acid, and lignan (Figure 5B) and docked to 6 key corresponding targets of the regulatory MAPK and PI3K/AKT pathways, including AKT1 (PDB ID: 3O96), BCL2 (PDB ID: 6O0K), GSK3β (PDB ID: 6B8J), MAPK1 (PDB ID: 2OJJ), MAPK14 (PDB ID: 1A9U) and TNF (PDB ID: 2AZ5). The predicted binding patterns are shown (Figure 5C–H). Among the necessary conditions for the pharmacological activity, hydrophobic interactions, π-cations, π-stacking, and conventional hydrogen bonding all have essential roles in protein-ligand recognition and stability and may be effective for the pharmacological activity.
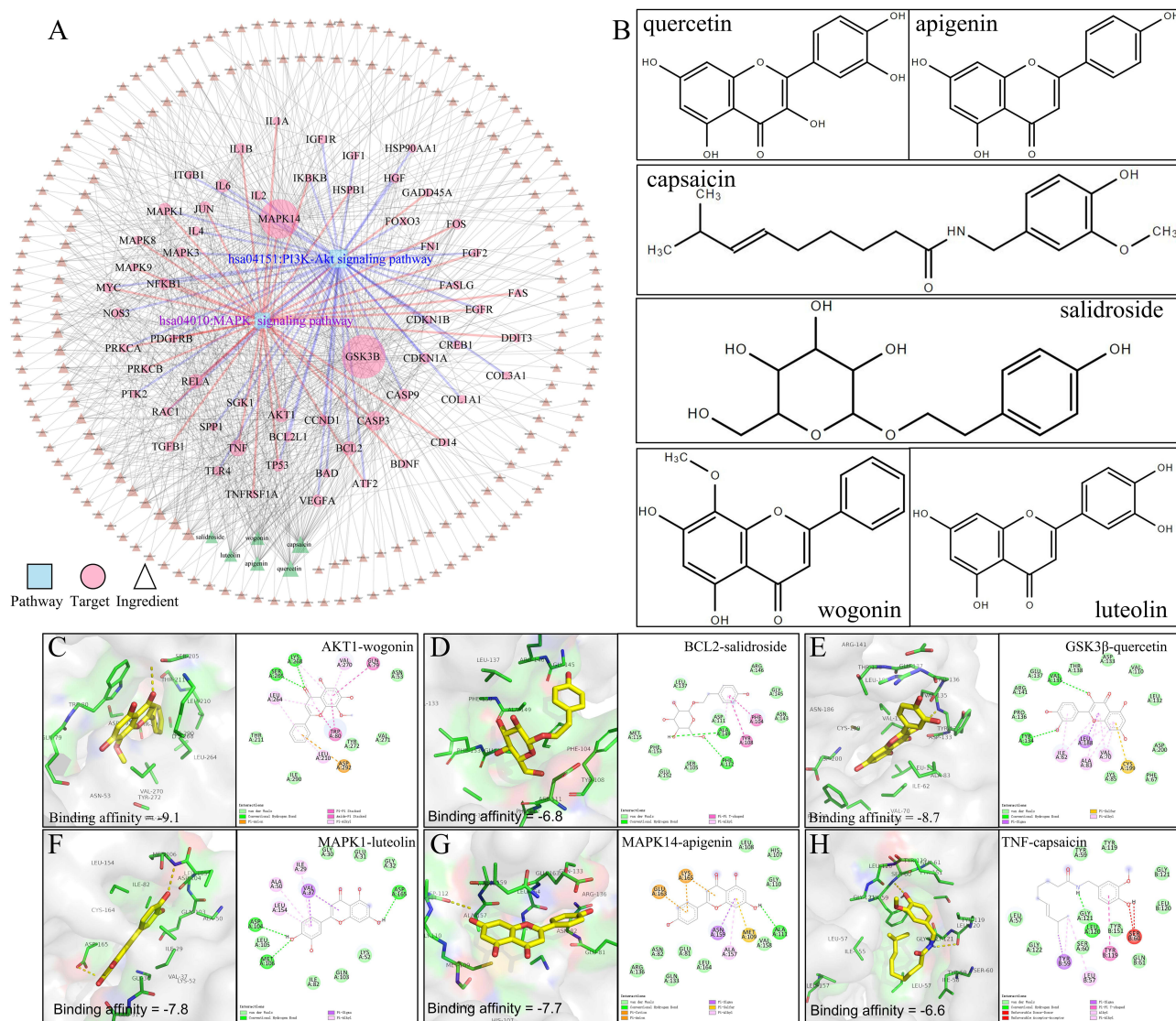
Figure 5 Molecular docking analysis of the core compounds of MBSYQ with key targets regulating MAPK and PI3K/AKT signaling pathways. Compound-target-pathway network (**A**), chemical structures of the six core compounds (**B**), predicted binding mode between AKT1 and wogonin (**C**), BCL2 and salidroside (**D**), GSK3β and quercetin (**E**), MAPK1 and luteolin (**F**), MAPK14 and apigenin (**G**), TNF and capsaicin (**H**). Cartoon patterns indicate protein binding, balls and bars indicate molecules, and lines indicate amino acid residues at the active site. The overall showed the two-dimensional and three-dimensional structure of the binding mode.

MBSYQ Alleviates Lung Inflammation and Airspace Enlargement Induced by Cigarette Smoke

After 24 weeks of CS exposure, lung histopathology of the control group showed normal lung structure, no inflammatory infiltration of small airways, and intact alveolar wall structure. In contrast, the lung tissue of the model group showed significant cellular infiltration with marked inflammation, small airway wall thickening, alveolar expansion, rupture, and parenchymal fusion, indicating successful induction of COPD-like responses in response to CS-exposure. In contrast, MBSYQ treatment improved the aforementioned histological changes, as demonstrated by a statistical decrease in inflammation scores, MLI, and MAA (Figure 6A–D). These results validate the efficiency of our animal model of COPD and the MBSYQ decoction treatment.
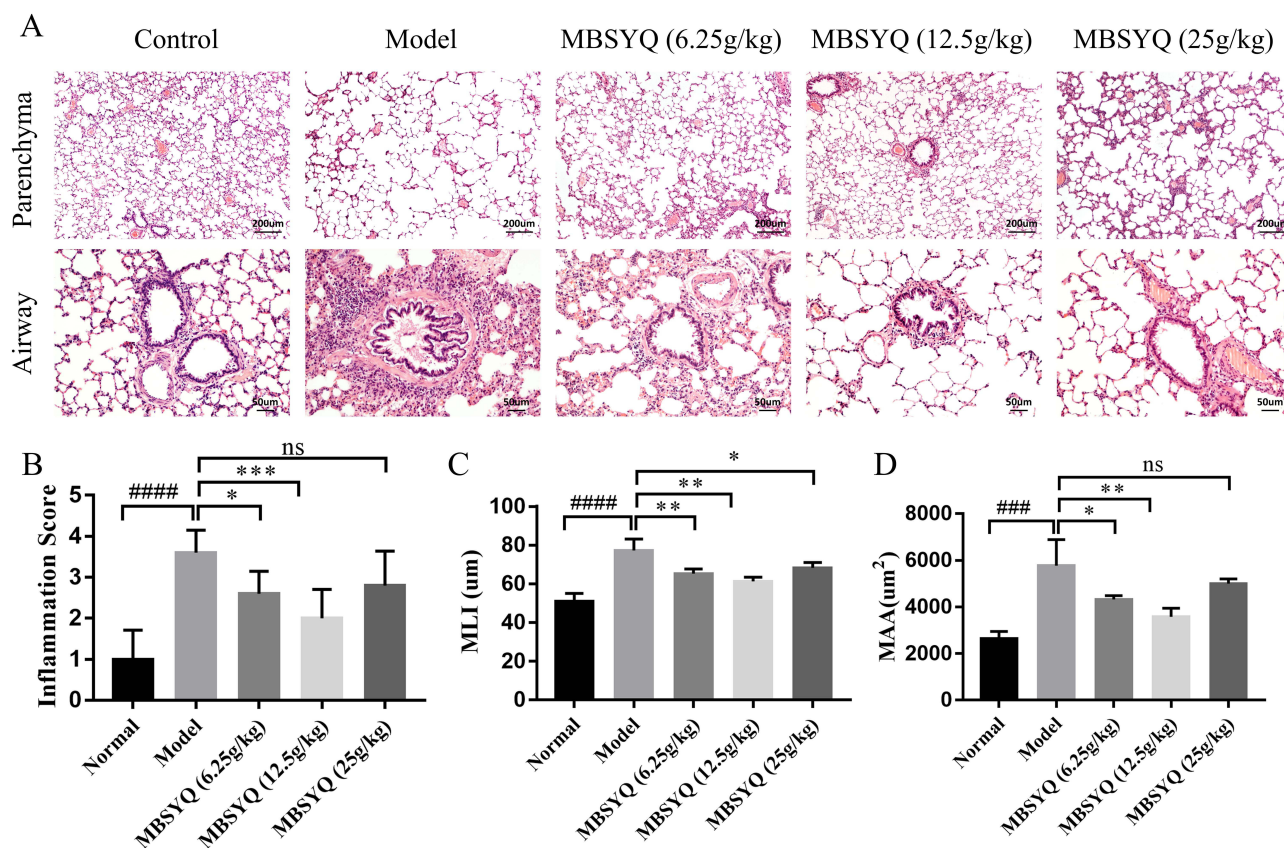
Figure 6 Cigarette smoking-induced lung inflammation and voids in rats can be attenuated by MBSYQ. (**A**) Lung section revealed by H&E staining. Alveolar inflammation scores (**B**), MLI (**C**), and MAA (**D**) were assessed. Data are presented as mean ± SD. ####p<0.0001, ###p<0.001 vs Control group; *p<0.05, **p<0.01, ***p<0.001 vs Model group.
Abbreviation: ns, no significance.

MBSYQ Restored the Femur/L1 Bone Mass and Microstructure Damage in CS-Exposure Rats

To further discover the role of MBSYQ in CS-exposed bone loss in rats, the bone microarchitecture of the distal femur and L1 was evaluated by Micro-CT, and representative scans are shown in Figure 7A. The CS-exposed group had a reduced number of bone trabeculae, a sparser distribution of bone trabeculae, and increased broken ends of bone trabeculae when compared to the control group. Quantitative analysis showed that BMD of the femur and L1 was obviously decreased in CS-exposure rats, and these changes were partially attenuated (not statistically significant) by MBSYQ (Figure 7B and C). Analysis of microstructural parameters revealed lower values of BV/TV (Figure 8A), BS/ TV (Figure 8B), Conn.D (Figure 8C), and Tb.N (Figure 8E) in the distal femur of CS-exposed rats compared to normal controls, while Tb.Sp (Figure 8D) was larger. However, these phenomena were partially reversed by MBSYQ (Figure 8A-E). There was no significant change in Tb.Th in all groups (Figure 8F). Our results suggest that 24 weeks of CS exposure can damage bone microstructure and that MBSYQ treatment is effective.

MBSYQ Upregulated Genes Associated with Anti-Oxidative Stress and Aerobic Respiration

To further explore the mechanism of MBSYQ on COPD-associated osteoporosis, we performed transcriptome sequencing analysis using rat tibial tissue. GO analysis of DEGs showed that the up-regulated genes were mainly related to oxygen metabolisms, such as aerobic respiration, oxidative phosphorylation, and detoxification of cellular oxidants, etc. (Figure 9A). These genes were up-regulated in the CS exposure group and further increased by MBSYQ (Figure 9B). We
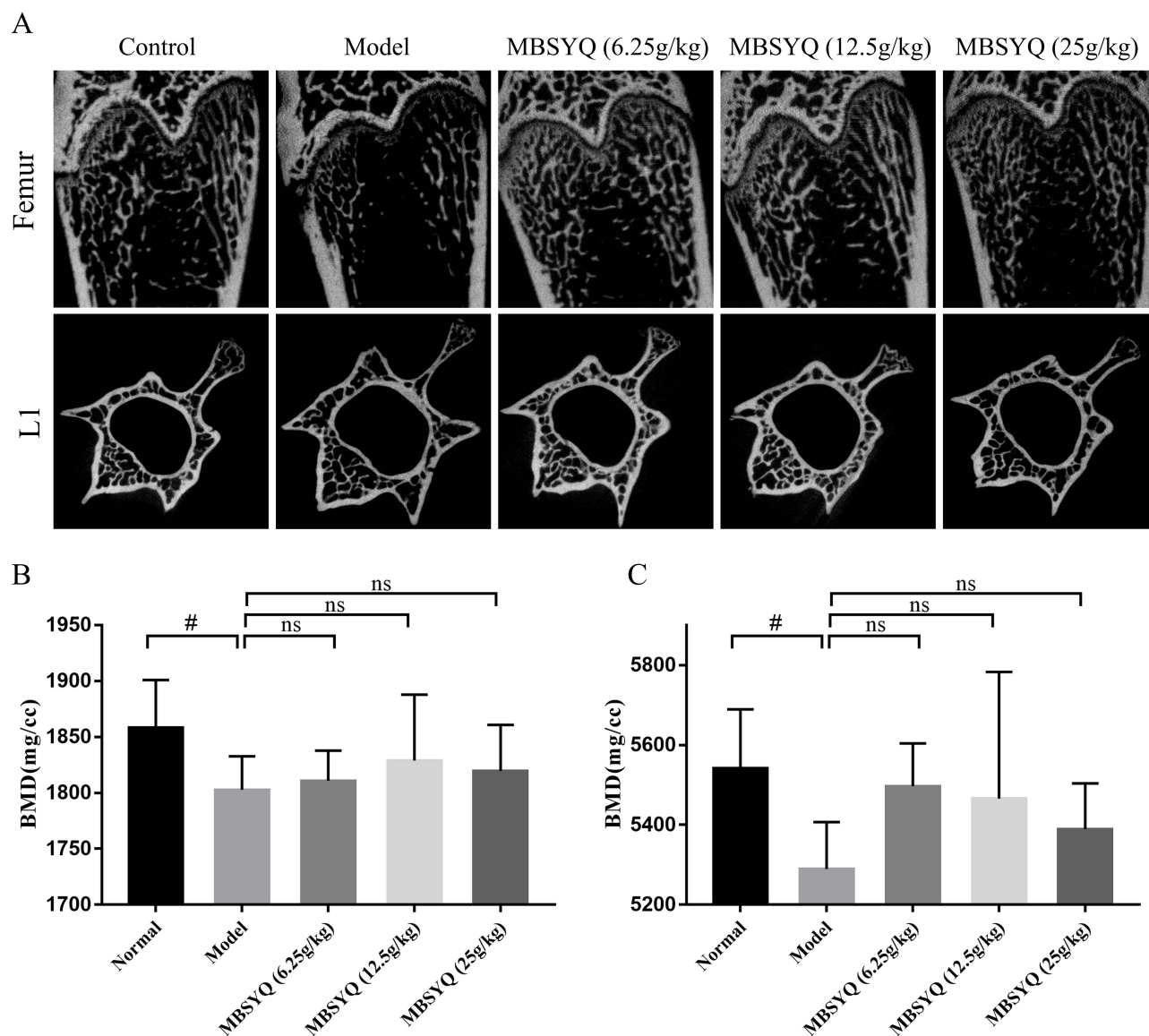
A

Figure 7 MBSYQ improves the BMD and bone microstructure of the femur and L1 induced by cigarette smoke. Representative scans of bone microstructure (**A**) and quantification of BMD of the femur (**B**) and L1 (**C**). #$p<0.05$ vs Control group.
Abbreviation: ns, no significance.

also constructed the associated PPI network and screened out the core genes ([Figure 9C](#)). The expressions of the core genes, including Gpx1, Gpx4, Ndufa4, and Uqcrb, were verified by RT-PCR experiment ([Figure 9D–G](#)). Gene expression trends were consistent with the RNA seq results, although sometimes the differences were not statistically significant. These results suggest an adaptive response to hypoxia during prolonged CS exposure and the efficiency of MBSYQ decoction therapy.

MAPK and PI3K/AKT Pathways Inhibited by CS Exposure Can Be Restored by MBSYQ

GSEA analysis showed that MAPK and PI3K/AKT signaling pathways were down-regulated in long-term CS exposure compared to the normal control group, while MBSYQ partially activated these signaling pathways ([Figure 10A–D](#)). This result was consistent with the consequence of network pharmacology ([Figure 4](#)). We further validated this result by
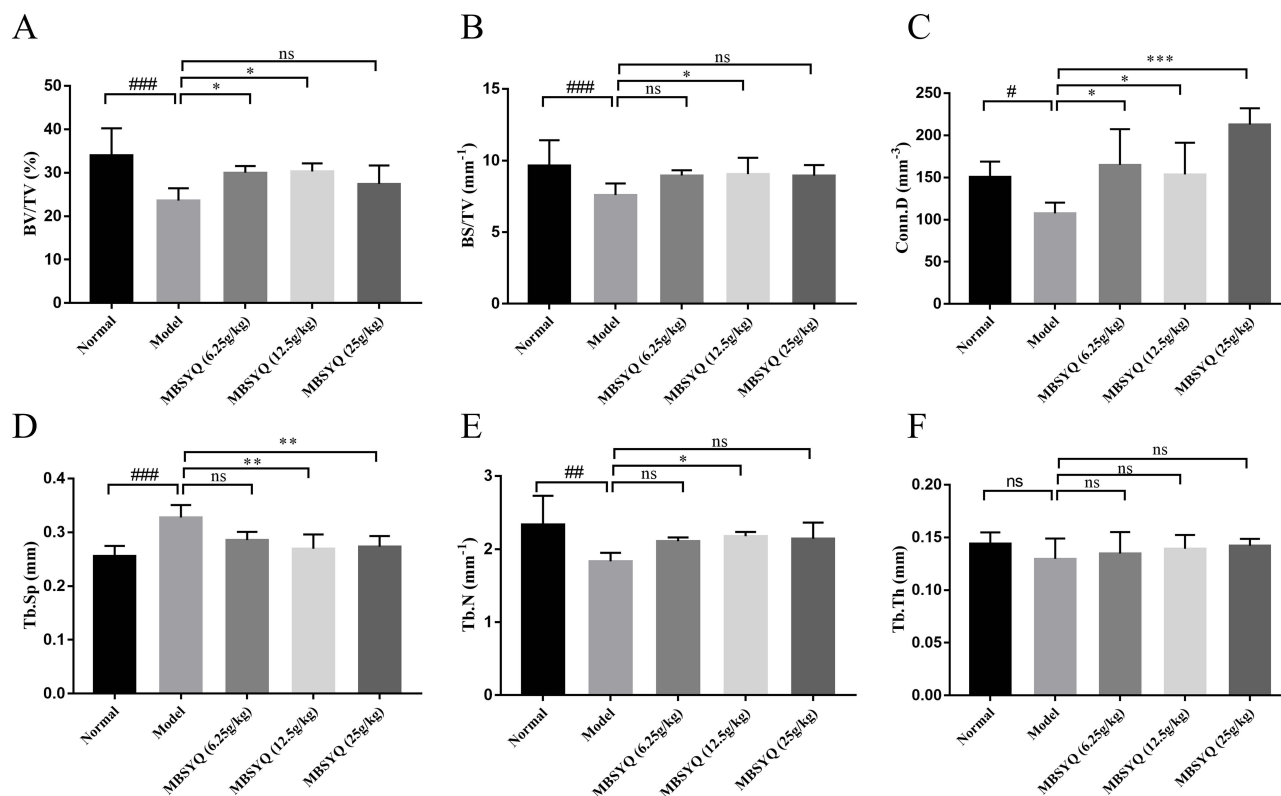
Figure 8 Quantitative analyses of trabecular parameters of the femur including. Micro-CT and Analyze12.0 were applied to determine the BV/TV (**A**), BS/TV (**B**), Conn.D (**C**), Tb.Sp (**D**), Tb.N (**E**), and Tb.Th (**F**). Data were expressed as mean ± SD. # $P < 0.05$, ## $P < 0.01$, ###$P < 0.001$ vs Control group. *$P < 0.05$, **$P < 0.01$, ***$P < 0.001$ vs CS exposure group.
Abbreviation: ns, no significance.

Western blot (Figure 10E–I). The expression of p-AKT, p-P38, p-JNK, and p-ERK was inhibited by CS exposure, which was partially reversed by MBSYQ.

Discussion

One of the common extra-pulmonary manifestations in COPD patients is osteoporosis, the probability of which is significantly higher than in the healthy population, and its severity is inversely correlated with bone mineral density. Cross-sectional studies based on COPD patients, population-based cohort studies, and the National Health and Nutrition Examination Survey (NHANES) have shown that the risk of COPD-related osteoporosis is approximately 1.5–2 times higher than that in control populations.[5–8,10] However, the underlying pathogenesis of COPD-related osteoporosis is still unclear and effective therapies are lacking. Here, we first attempted to elucidate the molecular link between COPD and osteoporosis and the potential mechanism of MBSYQ treatment. 340 common proteins were identified, and many COPD-related proteins belong to the same statistically significant GO terms and KEGG pathways as osteoporosis-specific proteins. 350 potential compounds from MBSYQ anchored 228 common targets for COPD-related osteoporosis treatment and showed modulation of MAPK and PI3K/AKT signaling pathways regulation. Then, we further employed a 24-week passive CS-exposed rat model to reveal the underlying mechanisms of COPD-associated osteoporosis and the therapeutic mechanism of MBSYQ. Here, we examined lung histopathology to assess the successful establishment of the COPD rat model and the therapeutic efficiency of MBSYQ. Then, we examined the microstructure of the distal femur and L1, demonstrating that MBSYQ can partially reverse the bone loss and microstructural damage in the femur and L1 induced by CS exposure. RNA sequencing can assist us in exploring the potential mechanisms of MBSYQ regulation. GSEA analysis revealed that MAPK and PI3K/AKT pathways were inhibited by CS exposure and activated by MBSYQ,
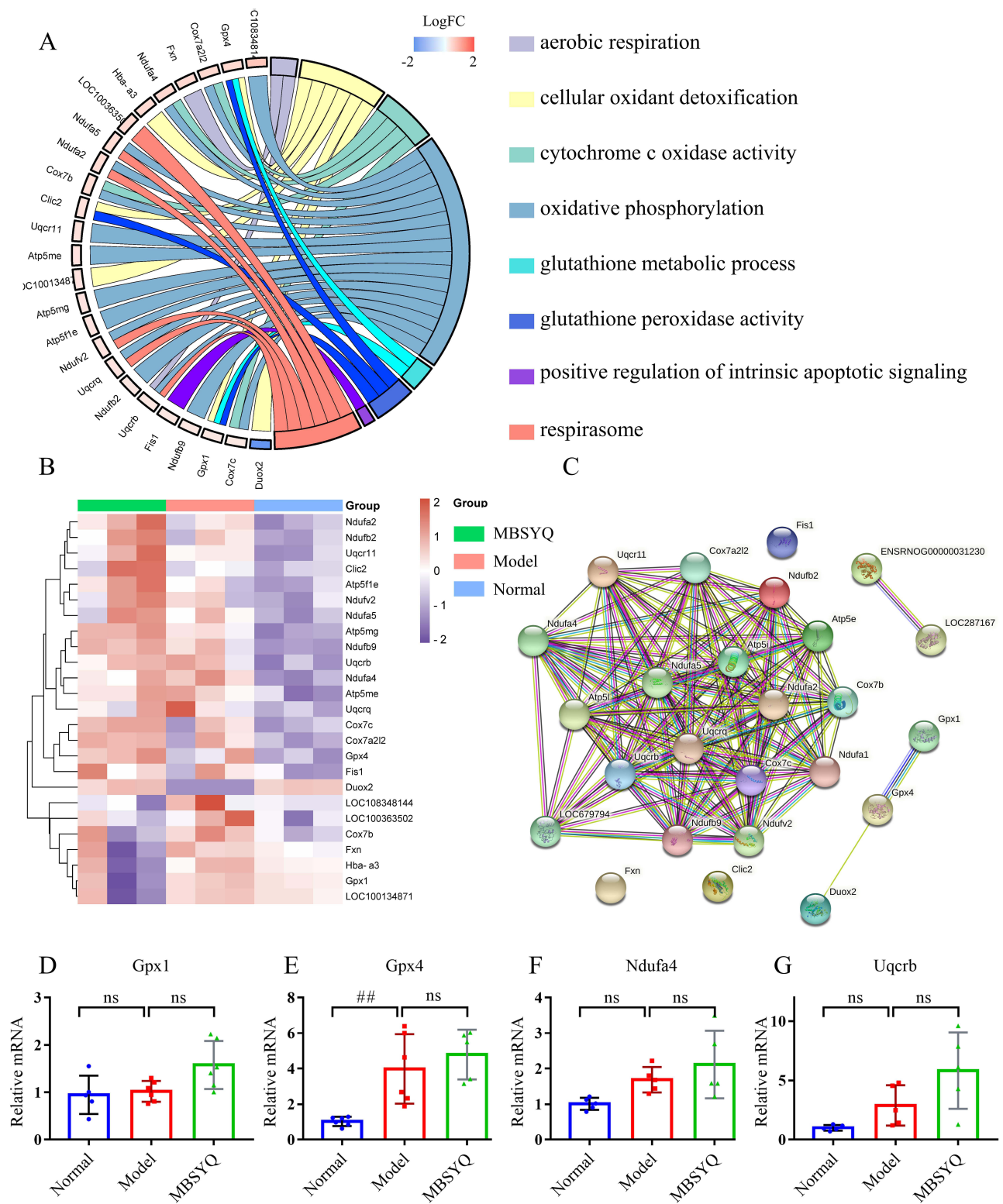
Figure 9 MBSYQ upregulates genes associated with anti-oxidative stress and aerobic respiration. GO Chord diagram of GO terms associated with oxygen metabolism and anti-oxidative stress (**A**), the heatmap of genes involved in the terms (**B**), and the PPI network of the genes (**C**). RT-PCR validation of core genes based on the PPI network, including GPX1 (**D**), GPX4 (**E**), Ndufa4 (**F**), and Uqcrb (**G**). ## P < 0.01 vs Control group.
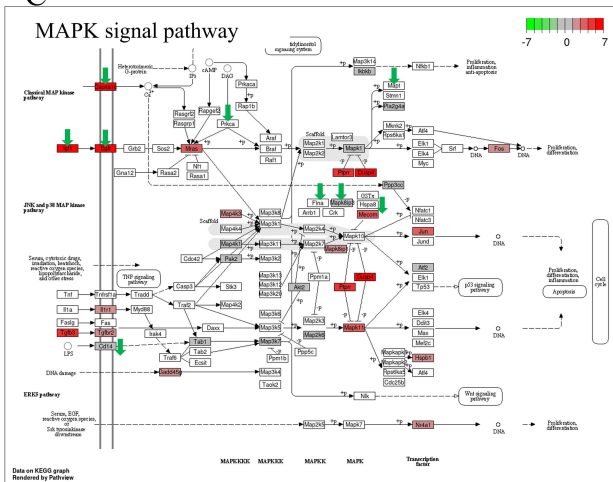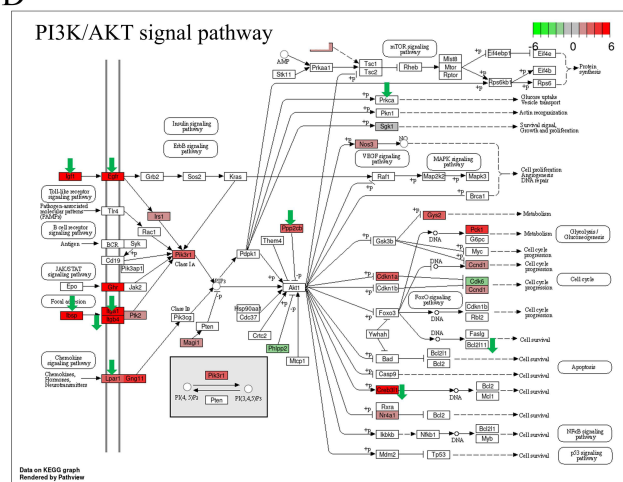**Abbreviation**: ns, no significance.
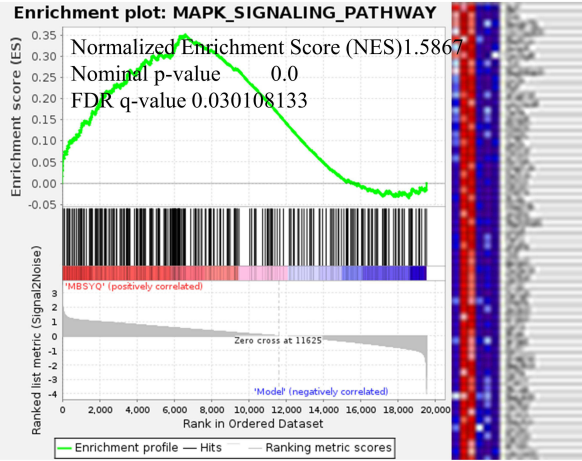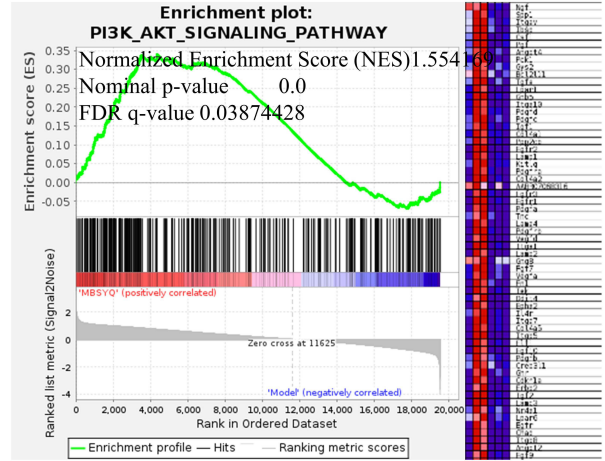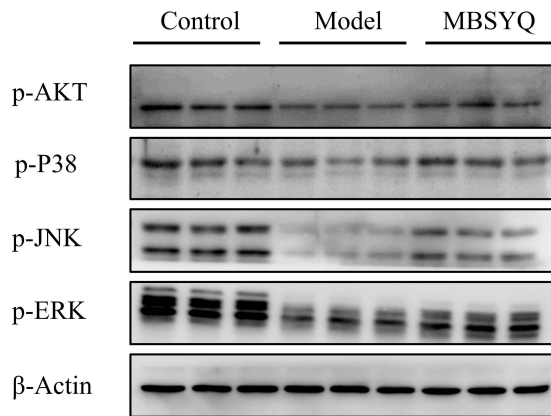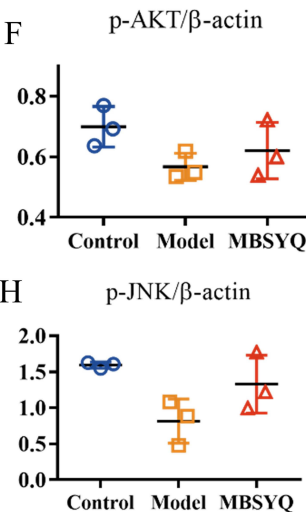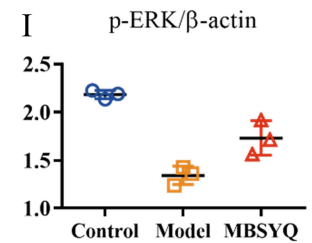
Figure 10 MBSYQ restored MAPK and PI3K/AKT pathways that were inhibited by cigarette exposure. GSEA enrichment showed that the MAPK pathway (**A*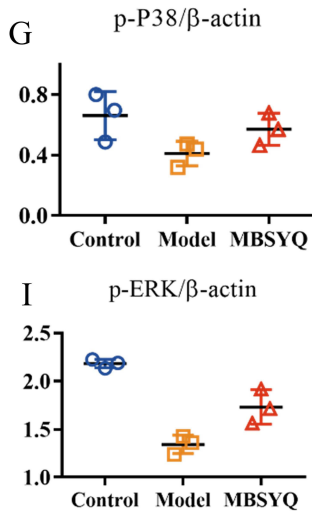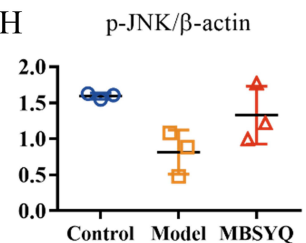*) and PI3K/ AKT (**B**) pathway were significantly activated by MBSYQ. Differentially expressed genes are labeled in the MAPK (**C**) and PI3K/AKT pathways (**D**); green arrows indicate genes down-regulated by CS exposure and red rectangles indicate genes up-regulated by MBSYQ. Western blot validated the relevant pathways in the normal, model, and MBSYQ groups (**E**) and Image-Pro Plus 6.0 for quantification of Western blot data (**F–I**).

which is consistent with network pharmacology predictions. The results suggest that MBSYQ is sufficient for the treatment of COPD-associated osteoporosis.

Interestingly, genes related to oxygen metabolism were significantly up-regulated by passive CS exposure and further up-regulated by MBSYQ. Previous studies have suggested that COPD patients suffer from chronic hypoxia due to the presence of irreversible airflow limitation and progressive decline in lung function. Chronic hypoxia inhibits the proliferation, differentiation, and mineralization of osteoblasts promotes their apoptosis, and inhibits the osteogenic function of bone marrow mesenchymal stem cells, while hypoxia is also an important stimulus for bone resorption. The concentration of hypoxia has a significant effect on the production and activity of osteoclasts, as the oxygen concentration decreases, the formation of osteoclast gradually increases, and more osteoclast nuclei are formed, but excessive hypoxia is detrimental to the growth of osteoclasts.[48] We found that chronic hypoxia in tibial tissues of CS-exposed rats resulted in the upregulation of genes related to oxidative phosphorylation and aerobic metabolism, which may be due to an intrinsic regulatory mechanism to improve the tolerance of the organism to hypoxia. The above genes were further up-regulated after MBSYQ treatment, indicating that MBSYQ further improved oxygen utilization efficiency and reduced oxidative stress damage induced by CS exposure.

The mitogen-activated protein kinase (MAPK) cascades are involved in cellular functions including cell proliferation, differentiation, and migration, and also have a critical role in skeletal homeostasis, and development, and is highly conserved. Inhibition of the JNK pathway by chemical inhibitors or siRNAs results in the downregulation of bone mineralization and several osteogenic markers; conversely, upregulation occurs when it activates the JNK pathway.[49] ERK1/2 is expressed in osteoblasts and has a relevant function in bone metabolism. Inhibition of ERK1/2 can impair osteoblast differentiation.[50] The deposition and mineralization of extracellular matrix, as well as the osteoblast differentiation response of osteogenic ligands (eg, TGF-β, BMP2, Wnt proteins, PTH, and epinephrine), can be regulated by the p38 MAPK pathway.[51–58] Our results suggest that MAPKs are inhibited by prolonged passive CS exposure, which impairs bone formation. Treatment with MBSYQ partially reverses this inhibition and ameliorates bone loss and bone microstructure damage. AKT is an essential serine/threonine protein kinase, which is relevant to many biological processes including metabolism, proliferation, cell survival, growth, and angiogenesis.[59–62] As the convergence and integration point of multiple stimuli related to the pathogenesis of COPD, AKT can be activated by a variety of inflammatory factors (such as TNF-α), growth factors (such as GM-CSF), and cigarette smoke components (such as nicotine),[63] thus improving the proliferation and survival of inflammatory cells such as macrophages, neutrophils, and T lymphocytes.[64] In addition, AKT has been associated with COPD-related systemic complications, such as skeletal muscle atrophy and metabolic disorder. Meanwhile, under normal conditions, the PI3K/AKT signaling pathway can selectively affect the physiological functions of osteoblasts and osteoclasts, promote the expression of markers of osteoblast differentiation such as alkaline phosphatase (ALP) and bone morphogenetic protein 2 (BMP-2), and promote the proliferation and differentiation of osteoblasts.[65] Rats deficient in AKT show insufficient bone growth in childhood and decreased bone mass in adulthood, suggesting their specific role in osteogenesis.[66] At the same time, PI3K/AKT signaling pathway participates in downstream RANK and macrophage colony-stimulating factor receptor (M-CSF) signals, thus playing a crucial role in osteoclast differentiation, survival, and bone resorption.[67] Inhibiting AKT can inhibit RANKL-induced osteoclast activation.[68] Therefore, they play different roles in regulating the survival and differentiation of osteoblasts and osteoclasts. AKT deficiency or inhibition of the PI3K/AKT pathway will cause changes in osteoblast bone formation and osteoclast bone resorption through their cellular self-aligning mechanisms. Previous studies have shown that activation of the PI3K/AKT pathway can enhance bone regeneration.[69] Here, we found that MBSYQ treatment could improve bone injury by activating the PI3K/Akt pathway.

Several limitations should be noted. First, the rats used in this study do not fully reflect the actual situation in humans, since the COPD model rats are young and have been gaining weight and growth throughout the experiment. In contrast, most human studies have been conducted on the elderly. Therefore, an animal model of COPD with older animals is worth testing. Second, the whole-body CS exposure model of COPD-related osteoporosis is inconsistent with the actual situation, which would increase the intake of nicotine, tar, and/or other cigarette substances. Therefore, further studies on nasal-only CS exposure models are needed.

Conclusion

The present work applied a network pharmacology approach combined with transcriptomics in a passive 24-week CS exposure rat model and found that MBSYQ was effective in the prevention and treatment of COPD-related osteoporosis, which was achieved in part through activation of MAPK and PI3K/AKT pathways. In clinical treatment, the present work provides valuable evidence for the application of MBSYQ in the treatment of COPD-related osteoporosis.

Abbreviations

COPD, chronic obstructive pulmonary disease; OP, osteoporosis; MBSYQD, modified Bu-Shen-Yi-Qi decoction; CS, cigarette smoke; TCM, traditional Chinese medicine; TTD, therapeutic target database; CTD, comparative toxicogenomics database; GO, gene ontology; KEGG, Kyoto Encyclopedia of Genes and Genomes; BP, biological process; CC, cellular component; MF, molecular function; H&E, hematoxylin-eosin; ELISA, enzyme-linked immunosorbent assay; DEGs, differentially expressed genes; BALF, bronchoalveolar lavage fluid; PPI, protein-protein interaction.

Data Sharing Statement

The raw data of RNA seq presented in this study can be found in the online repository (https://dataview.ncbi.nlm.nih.gov/object/PRJNA818808?reviewer=gh364b75ugd2bqshl94q6thlua). The other data used to support the findings of this study are included within the article and the supplementary files, further available from the corresponding authors on reasonable request.

Ethics Approval and Informed Consent

This study was reviewed and approved by the Institutional Review board of Huashan Hospital, Fudan university (HIRB). Animal experiments were approved by the Animal Experimentation Ethics Committee of Fudan University (Approval No. 202011005S) and were performed in accordance with the principles outlined in the Guide for the Care and Use of Laboratory Animals published by the National Institutes of Health (NIH).

Author Contributions

All authors made a significant contribution to the work reported, whether that is in the conception, study design, execution, acquisition of data, analysis and interpretation, or in all these areas; took part in drafting, revising or critically reviewing the article; gave final approval of the version to be published; have agreed on the journal to which the article has been submitted; and agree to be accountable for all aspects of the work.

Funding

Disclosure

The authors report no conflicts of interest in this work.

References

1. Lozano R, Naghavi M, Foreman K, et al. Global and regional mortality from 235 causes of death for 20 age groups in 1990 and 2010: a systematic analysis for the global burden of disease study 2010. *Lancet*. 2012;380(9859):2095–2128. doi:10.1016/S0140-6736(12)61728-0

2. Lehouck A, Boonen S, Decramer M, Janssens W. COPD, bone metabolism, and osteoporosis. *Chest*. 2011;139(3):648–657. doi:10.1378/chest.10-1427

3. Decramer M, Rennard S, Troosters T, et al. COPD as a lung disease with systemic consequences--clinical impact, mechanisms, and potential for early intervention. *Copd*. 2008;5(4):235–256. doi:10.1080/15412550802237531

4. Decramer M, Janssens W. Chronic obstructive pulmonary disease and comorbidities. *Lancet Respir Med*. 2013;1(1):73–83. doi:10.1016/S2213-2600(12)70060-7

5. Bolton CE, Ionescu AA, Shiels KM, et al. Associated loss of fat-free mass and bone mineral density in chronic obstructive pulmonary disease. *Am J Respir Crit Care Med*. 2004;170(12):1286–1293. doi:10.1164/rccm.200406-754OC

6. Sabit R, Bolton CE, Edwards PH, et al. Arterial stiffness and osteoporosis in chronic obstructive pulmonary disease. *Am J Respir Crit Care Med*. 2007;175(12):1259–1265. doi:10.1164/rccm.200701-067OC

7. Dam TT, Harrison S, Fink HA, Ramsdell J, Barrett-Connor E. Bone mineral density and fractures in older men with chronic obstructive pulmonary disease or asthma. *Osteoporos Int*. 2010;21(8):1341–1349. doi:10.1007/s00198-009-1076-x

8. Chen SJ, Liao WC, Huang KH, et al. Chronic obstructive pulmonary disease and allied conditions is a strong independent risk factor for osteoporosis and pathologic fractures: a population-based cohort study. *QJM*. 2015;108(8):633–640. doi:10.1093/qjmed/hcv012

9. Kjensli A, Mowinckel P, Ryg MS, Falch JA. Low bone mineral density is related to severity of chronic obstructive pulmonary disease. *Bone*. 2007;40(2):493–497. doi:10.1016/j.bone.2006.09.005

10. Schnell K, Weiss CO, Lee T, et al. The prevalence of clinically-relevant comorbid conditions in patients with physician-diagnosed COPD: a cross-sectional study using data from NHANES 1999-2008. *BMC Pulm Med*. 2012;12:26. doi:10.1186/1471-2466-12-26

11. Ryan CS, Petkov VI, Adler RA. Osteoporosis in men: the value of laboratory testing. *Osteoporos Int*. 2011;22(6):1845–1853. doi:10.1007/s00198-010-1421-0

12. Barnes PJ. Mediators of chronic obstructive pulmonary disease. *Pharmacol Rev*. 2004;56(4):515–548. doi:10.1124/pr.56.4.2

13. Raisz LG. Pathogenesis of osteoporosis: concepts, conflicts, and prospects. *J Clin Invest*. 2005;115(12):3318–3325. doi:10.1172/JCI27071

14. Watanabe R, Tanaka T, Aita K, et al. Osteoporosis is highly prevalent in Japanese males with chronic obstructive pulmonary disease and is associated with deteriorated pulmonary function. *J Bone Miner Metab*. 2015;33(4):392–400. doi:10.1007/s00774-014-0605-7

15. Tsukamoto M, Mori T, Wang KY, et al. Systemic bone loss, impaired osteogenic activity and type I muscle fiber atrophy in mice with elastase-induced pulmonary emphysema: establishment of a COPD-related osteoporosis mouse model. *Bone*. 2019;120:114–124. doi:10.1016/j.bone.2018.10.017

16. Sarkar M, Bhardwaj R, Madabhavi I, Khatana J. Osteoporosis in chronic obstructive pulmonary disease. *Clin Med Insights Circ Respir Pulm Med*. 2015;9:5–21. doi:10.4137/CCRPM.S22803

17. Graat-Verboom L, van den Borne BE, Smeenk FW, Spruit MA, Wouters EF. Osteoporosis in COPD outpatients based on bone mineral density and vertebral fractures. *J Bone Miner Res*. 2011;26(3):561–568. doi:10.1002/jbmr.257

18. Compston JE, McClung MR, Leslie WD. Osteoporosis. *Lancet*. 2019;393(10169):364–376. doi:10.1016/S0140-6736(18)32112-3

19. Rodan GA, Martin TJ. Therapeutic approaches to bone diseases. *Science*. 2000;289(5484):1508–1514. doi:10.1126/science.289.5484.1508

20. Jiang Y, Zhang P, Zhang X, Lv L, Zhou Y. Advances in mesenchymal stem cell transplantation for the treatment of osteoporosis. *Cell Prolif*. 2021;54(1):e12956. doi:10.1111/cpr.12956

21. Jiang TM. Identification of the genetic central dogma in osteogenic differentiation of MSCs by osteoinductive medium from transcriptional data sets. *Chronic Dis Transl Med*. 2022;8(3):218–228. doi:10.1002/cdt3.26

22. Kong DX, Li XJ, Zhang HY. Where is the hope for drug discovery? Let history tell the future. *Drug Discov Today*. 2009;14(3–4):115–119. doi:10.1016/j.drudis.2008.07.002

23. Cheung F. TCM: made in China. *Nature*. 2011;480(7378):S82–83. doi:10.1038/480S82a

24. Zhong Y, Luo J, Tang T, et al. Exploring pharmacological mechanisms of Xuefu Zhuyu decoction in the treatment of traumatic brain injury via a network pharmacology approach. *Evid Based Complementary Altern Med*. 2018;2018:8916938. doi:10.1155/2018/8916938

25. Cui J, Xu F, Tang Z, et al. Bu-Shen-Yi-Qi formula ameliorates airway remodeling in murine chronic asthma by modulating airway inflammation and oxidative stress in the lung. *Biomed Pharmacother*. 2019;112:108694. doi:10.1016/j.biopha.2019.108694

26. Wei Y, Luo QL, Sun J, Chen MX, Liu F, Dong JC. Bu-Shen-Yi-Qi formulae suppress chronic airway inflammation and regulate Th17/Treg imbalance in the murine ovalbumin asthma model. *J Ethnopharmacol*. 2015;164:368–377. doi:10.1016/j.jep.2015.01.016

27. Wang G, Liu B, Cao Y, et al. Effects of two Chinese herbal formulae for the treatment of moderate to severe stable chronic obstructive pulmonary disease: a multicenter, double-blind, randomized controlled trial. *PLoS One*. 2014;9(8):e103168. doi:10.1371/journal.pone.0103168

28. Kong L, Zhang H, Cao Y, et al. The anti-inflammatory effects of invigorating kidney and supplementing Qi Chinese Herbal formulae in asthma patients. *Evid Based Complementary Altern Med*. 2017;2017:3754145. doi:10.1155/2017/3754145

29. Kong Q, Mo S, Wang W, et al. Efficacy and safety of Jia Wei Bushen Yiqi formulas as an adjunct therapy to systemic glucocorticoids on acute exacerbation of COPD: study protocol for a randomized, double-blinded, multi-center, placebo-controlled clinical trial. *Trials*. 2020;21(1):760. doi:10.1186/s13063-020-04669-5

30. Wang Y, Zhang S, Li F, et al. Therapeutic target database 2020: enriched resource for facilitating research and early development of targeted therapeutics. *Nucleic Acids Res*. 2020;48(D1):D1031–d1041. doi:10.1093/nar/gkz981

31. Davis AP, Grondin CJ, Johnson RJ, et al. Comparative Toxicogenomics Database (CTD): update 2021. *Nucleic Acids Res*. 2021;49(D1):D1138–d1143. doi:10.1093/nar/gkaa891

32. Piñero J, Ramírez-Anguita JM, Saüch-Pitarch J, et al. The DisGeNET knowledge platform for disease genomics: 2019 update. *Nucleic Acids Res*. 2020;48(D1):D845–d855. doi:10.1093/nar/gkz1021

33. Fang S, Dong L, Liu L, et al. HERB: a high-throughput experiment- and reference-guided database of traditional Chinese medicine. *Nucleic Acids Res*. 2021;49(D1):D1197–d1206. doi:10.1093/nar/gkaa1063

34. Hecker N, Ahmed J, von Eichborn J, et al. SuperTarget goes quantitative: update on drug-target interactions. *Nucleic Acids Res*. 2012;40:D1113–1117. doi:10.1093/nar/gkr912

35. Daina A, Michielin O, Zoete V. SwissTargetPrediction: updated data and new features for efficient prediction of protein targets of small molecules. *Nucleic Acids Res*. 2019;47(W1):W357–w364. doi:10.1093/nar/gkz382

36. Keiser MJ, Roth BL, Armbruster BN, Ernsberger P, Irwin JJ, Shoichet BK. Relating protein pharmacology by ligand chemistry. *Nat Biotechnol*. 2007;25(2):197–206. doi:10.1038/nbt1284

37. Szklarczyk D, Santos A, von Mering C, Jensen LJ, Bork P, Kuhn M. STITCH 5: augmenting protein-chemical interaction networks with tissue and affinity data. *Nucleic Acids Res*. 2016;44(D1):D380–384. doi:10.1093/nar/gkv1277

38. Wang X, Shen Y, Wang S, et al. PharmMapper 2017 update: a web server for potential drug target identification with a comprehensive target pharmacophore database. *Nucleic Acids Res*. 2017;45(W1):W356–w360. doi:10.1093/nar/gkx374

39. Shannon P, Markiel A, Ozier O, et al. Cytoscape: a software environment for integrated models of biomolecular interaction networks. *Genome Res*. 2003;13(11):2498–2504. doi:10.1101/gr.1239303

40. Huang da W, Sherman BT, Lempicki RA. Systematic and integrative analysis of large gene lists using DAVID bioinformatics resources. *Nat Protoc*. 2009;4(1):44–57. doi:10.1038/nprot.2008.211

41. Zhou Y, Zhou B, Pache L, et al. Metascape provides a biologist-oriented resource for the analysis of systems-level datasets. *Nat Commun*. 2019;10 (1):1523. doi:10.1038/s41467-019-09234-6

42. Nair AB, Jacob S. A simple practice guide for dose conversion between animals and human. *J Basic Clin Pharm*. 2016;7(2):27–31. doi:10.4103/0976-0105.177703

43. Zhang H, Liu B, Jiang S, et al. Baicalin ameliorates cigarette smoke-induced airway inflammation in rats by modulating HDAC2/NF-κB/PAI-1 signalling. *Pulm Pharmacol Ther*. 2021;70:102061. doi:10.1016/j.pupt.2021.102061

44. Li Q, Wang G, Xiong SH, et al. Bu-Shen-Fang-Chuan formula attenuates cigarette smoke-induced inflammation by modulating the PI3K/Akt-Nrf2 and NF-κB signalling pathways. *J Ethnopharmacol*. 2020;261:113095. doi:10.1016/j.jep.2020.113095

45. Wang G, Mohammadtursun N, Sun J, et al. Establishment and evaluation of a rat model of sidestream cigarette smoke-induced chronic obstructive pulmonary disease. *Front Physiol*. 2018;9:58. doi:10.3389/fphys.2018.00058

46. Shen HH, Wang K, Li W, et al. Astragalus Membranaceus prevents airway hyperreactivity in mice related to Th2 response inhibition. *J Ethnopharmacol*. 2008;116(2):363–369. doi:10.1016/j.jep.2007.12.002

47. Song X, Wang C, Bai C. Establishment of rat chronic obstructive pulmonary disease model: a comparison between exposure to cigarette smoke alone and in combination with intra-tracheal injection of lipopolysaccharide. *Acad J Second Mil Med Univ*. 2010;31(03):246–249.

48. Fukuoka H, Aoyama M, Miyazawa K, Asai K, Goto S. Hypoxic stress enhances osteoclast differentiation via increasing IGF2 production by non-osteoclastic cells. *Biochem Biophys Res Commun*. 2005;328(4):885–894. doi:10.1016/j.bbrc.2005.01.042

49. Liu H, Liu Y, Viggeswarapu M, Zheng Z, Titus L, Boden SD. Activation of c-Jun NH(2)-terminal kinase 1 increases cellular responsiveness to BMP-2 and decreases binding of inhibitory Smad6 to the type 1 BMP receptor. *J Bone Miner Res*. 2011;26(5):1122–1132. doi:10.1002/jbmr.296

50. Matsushita T, Chan YY, Kawanami A, Balmes G, Landreth GE, Murakami S. Extracellular signal-regulated kinase 1 (ERK1) and ERK2 play essential roles in osteoblast differentiation and in supporting osteoclastogenesis. *Mol Cell Biol*. 2009;29(21):5843–5857. doi:10.1128/MCB.01549-08

51. Lai CF, Cheng SL. Signal transductions induced by bone morphogenetic protein-2 and transforming growth factor-beta in normal human osteoblastic cells. *J Biol Chem*. 2002;277(18):15514–15522. doi:10.1074/jbc.M200794200

52. Guicheux J, Lemonnier J, Ghayor C, Suzuki A, Palmer G, Caverzasio J. Activation of p38 mitogen-activated protein kinase and c-Jun-NH2-terminal kinase by BMP-2 and their implication in the stimulation of osteoblastic cell differentiation. *J Bone Miner Res*. 2003;18(11):2060–2068. doi:10.1359/jbmr.2003.18.11.2060

53. Nöth U, Tuli R, Seghatoleslami R, et al. Activation of p38 and Smads mediates BMP-2 effects on human trabecular bone-derived osteoblasts. *Exp Cell Res*. 2003;291(1):201–211. doi:10.1016/S0014-4827(03)00386-0

54. Caverzasio J, Manen D. Essential role of Wnt3a-mediated activation of mitogen-activated protein kinase p38 for the stimulation of alkaline phosphatase activity and matrix mineralization in C3H10T1/2 mesenchymal cells. *Endocrinology*. 2007;148(11):5323–5330. doi:10.1210/en.2007-0520

55. Chang J, Sonoyama W, Wang Z, et al. Noncanonical Wnt-4 signaling enhances bone regeneration of mesenchymal stem cells in craniofacial defects through activation of p38 MAPK. *J Biol Chem*. 2007;282(42):30938–30948. doi:10.1074/jbc.M702391200

56. Rey A, Manen D, Rizzoli R, Ferrari SL, Caverzasio J. Evidences for a role of p38 MAP kinase in the stimulation of alkaline phosphatase and matrix mineralization induced by parathyroid hormone in osteoblastic cells. *Bone*. 2007;41(1):59–67. doi:10.1016/j.bone.2007.02.031

57. Bianchi EN, Ferrari SL. Beta-arrestin2 regulates parathyroid hormone effects on a p38 MAPK and NFkappaB gene expression network in osteoblasts. *Bone*. 2009;45(4):716–725. doi:10.1016/j.bone.2009.06.020

58. Suzuki A, Palmer G, Bonjour JP, Caverzasio J. Regulation of alkaline phosphatase activity by p38 MAP kinase in response to activation of Gi protein-coupled receptors by epinephrine in osteoblast-like cells. *Endocrinology*. 1999;140(7):3177–3182. doi:10.1210/endo.140.7.6857

59. Heron-Milhavet L, Khouya N, Fernandez A, Lamb NJ. Akt1 and Akt2: differentiating the aktion. *Histol Histopathol*. 2011;26(5):651–662. doi:10.14670/HH-26.651

60. Hers I, Vincent EE, Tavaré JM. Akt signalling in health and disease. *Cell Signal*. 2011;23(10):1515–1527. doi:10.1016/j.cellsig.2011.05.004

61. Nicholson KM, Anderson NG. The protein kinase B/Akt signalling pathway in human malignancy. *Cell Signal*. 2002;14(5):381–395. doi:10.1016/S0898-6568(01)00271-6

62. Rönnstrand L. Signal transduction via the stem cell factor receptor/c-Kit. *Cell Mol Life Sci*. 2004;61(19–20):2535–2548. doi:10.1007/s00018-004-4189-6

63. Bozinovski S, Vlahos R, Hansen M, Liu K, Anderson GP. Akt in the pathogenesis of COPD. *Int J Chron Obstruct Pulmon Dis*. 2006;1(1):31–38. doi:10.2147/copd.2006.1.1.31

64. Jones RG, Parsons M, Bonnard M, et al. Protein kinase B regulates T lymphocyte survival, nuclear factor kappaB activation, and Bcl-X(L) levels in vivo. *J Exp Med*. 2000;191(10):1721–1734. doi:10.1084/jem.191.10.1721

65. Wu CM, Chen PC, Li TM, Fong YC, Tang CH. Si-Wu-tang extract stimulates bone formation through PI3K/Akt/NF-κB signaling pathways in osteoblasts. *BMC Complement Altern Med*. 2013;13:277. doi:10.1186/1472-6882-13-277

66. Peng XD, Xu PZ, Chen ML, et al. Dwarfism, impaired skin development, skeletal muscle atrophy, delayed bone development, and impeded adipogenesis in mice lacking Akt1 and Akt2. *Genes Dev*. 2003;17(11):1352–1365. doi:10.1101/gad.1089403

67. Adapala NS, Barbe MF, Tsygankov AY, Lorenzo JA, Sanjay A. Loss of Cbl-PI3K interaction enhances osteoclast survival due to p21-Ras mediated PI3K activation independent of Cbl-b. *J Cell Biochem*. 2014;115(7):1277–1289. doi:10.1002/jcb.24779

68. Yu L, Jia D, Feng K, et al. A natural compound (LCA) isolated from Litsea cubeba inhibits RANKL-induced osteoclast differentiation by suppressing Akt and MAPK pathways in mouse bone marrow macrophages. *J Ethnopharmacol*. 2020;257:112873. doi:10.1016/j.jep.2020.112873

69. Zhang J, Liu X, Li H, et al. Exosomes/tricalcium phosphate combination scaffolds can enhance bone regeneration by activating the PI3K/Akt signaling pathway. *Stem Cell Res Ther*. 2016;7(1):136. doi:10.1186/s13287-016-0391-3